Validating GOES Active Fire Detection Product Using ASTER and ETM+

Wilfrid Schroeder[1], Ivan Csiszar[1], Elaine Prins[2], Chris Schmidt[2] & Mark Ruminski[3]*

[1] Department of Geography University of Maryland, [2] CIMSS University of Wisconsin, [3] Satellite Applications Branch NOAA/NESDIS

[*] Corresponding Author, Email: schroeder@hermes.geog.umd.edu

Introduction

Vegetation fires, in combination with deforestation activities, result in the conversion and the alteration of large areas of evergreen tropical forests, transitional forests and savanna vegetation throughout the tropics each year [Cochrane et al., 1999]. Their importance is also rapidly increasing in regions where the proximity to urban areas can result in large populations directly impacted by such events [Keeley *et al*., 1999]. Important areas of intense fire activity in the tropics include the Arc of Deforestation across Brazilian Amazonia [Schroeder *et al*., 2005; Setzer and Pereira, 1991], whereas the large California shrubland fires constitutes one of the most clear examples of wildfires affecting large urban areas in recent years. That places the Americas under the spotlight in terms of vegetation fire activity globally.

The GOES imager provides regular active fire detection data for the Americas at high observation frequency [CIMSS, 2007; Prins and Menzel,1994], serving as an important tool for fire managing groups as well as for emissions modellers [CPTEC, 2007 ; Freitas *et al*., 2005; HMS, 2007]. Accurate and consistent fire detection data becomes essential in this case to assess the affected areas during emergency situations as well as to generate reliable forecast of smoke plume transport and biomass burning emissions estimates.

In this study we validate the Wildfire Automated Biomass Burning Algorithm (WFABBA) generated by the Cooperative Institute for Meteorological Satellite Studies (CIMSS) at the University of Wisconsin, Madison, using a large selection of 30 m resolution data from the Advanced Spaceborne Thermal Emission and Reflection Radiometer (ASTER) and the Landsat 7 Enhanced Thematic Mapper Plus (ETM+). We establish the overall WFABBA detection envelope using 30 m active fire statistics at the GOES pixel level and we report the commission and omission errors for the product. Major elements affecting the performance of the WFABBA are highlighted.

In the last section, we compare the results produced from WFABBA to the 1×1 km resolution *Thermal Anomalies* (MOD14) product derived from the Moderate Resolution Imaging Spectroradiometer (MODIS) on board the Terra satellite. We summarize the main differences and similarities between the two products.

Data & Methods

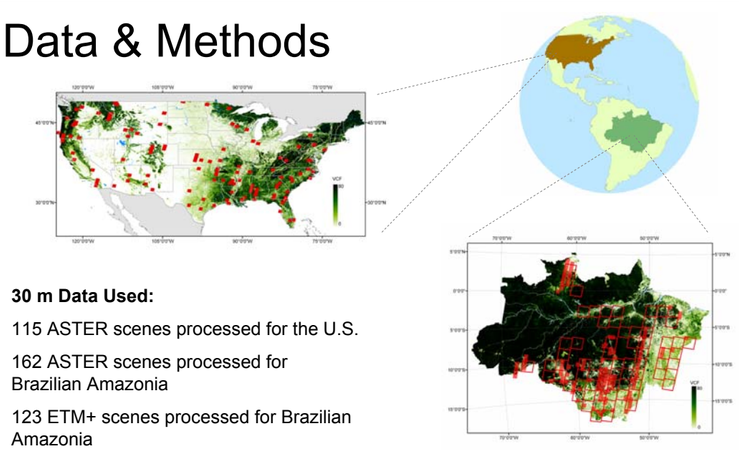

30 m Data Used:

115 ASTER scenes processed for the U.S.

162 ASTER scenes processed for Brazilian Amazonia

123 ETM+ scenes processed for Brazilian Amazonia

Figure 1: ASTER (shaded red areas) and ETM+ (open red areas) scenes utilized to validate the WFABBA product over the conterminous U.S. and Brazilian Amazonia.

GOES Data Sampled:

U.S.: 3,300 GOES pixels with at least one 30 m fire pixel, 102 fire detections produced

Brazilian Amazonia: 17,400 GOES pixels with at least one 30 m fire pixel, 560 fire detections produced

Methods:

- GOES data selected within ±15 min of the ASTER and ETM+ scenes
- All GOES data used were registered to <1 pixel
- Active fire masks were derived from the 30 m resolution imagery to serve as our validation data [Giglio et *al*., 2008; Schroeder *et al*., 2008]
- Logistic regression analysis used to derive detection envelopes by relating 30 m fire statistics to GOES pixel area [Morisette *et al*., 2005, Csiszar *et al*., 2006]
- Error matrix analysis used to derive commission and omission errors

Results

Detection Probability

Logistic regression analysis was used to determine the detection probability of WFABBA. The regression model relates the number of 30 m active fire pixels contained within the GOES footprint to WFABBA fire detections (i.e., true positives).

Detection probability curves derived for four percentage tree cover intervals across Brazilian Amazonia [for VCF reference, see Hansen *et al*., 2002].

Higher detection rates were sistematically found for high percentage tree cover areas. This finding is explained by the occurrence of higher intensity fires as a result of increased biomass loads relatively to low percentage tree cover areas.

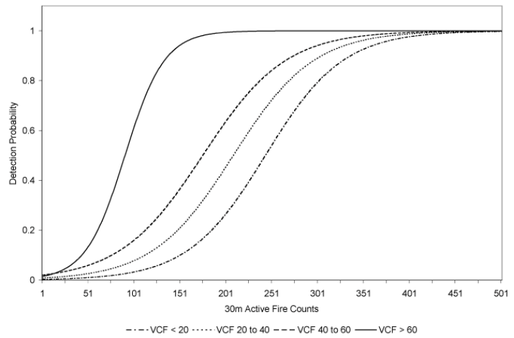

Figure 2: Detection probability derived for the WFABBA product over Brazilian Amazonia. Detection curves are plotted separately for different percentage tree cover intervals based on the Vegetation Continuous Fields product (VCF; Hansen et al., 2002)

Omission Errors

Error matrix analysis was used to determine the omission error estimates for WFABBA at approximately 1030 local time. In this case, we counted the number of WFABBA detections for each subset of GOES pixels showing a number of 30 m active fire pixels greater or equal to *N*. Omission errors were produced by varying *N* between 1 and the maximum value in our data set (~1,200).

Omission error estimates were produced for the standard WFABBA product as well as for the product without the temporal filter analysis applied (a test to eliminate spurious detections).

The WFABBA daytime detection omission error estimate for all fires mapped with the 30 m resolution data was also determined by using all available observations until 2000 local time.

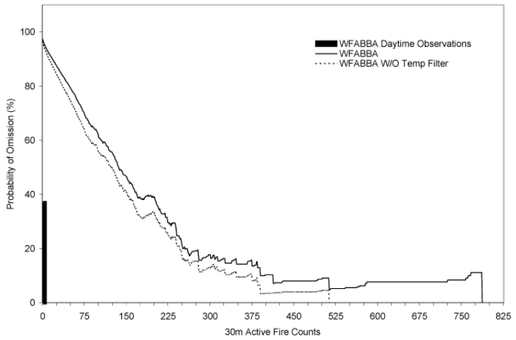

Figure 3: Omission error estimates derived from the WFABBA product over Brazilian Amazonia. Solid line corresponds to the standard WFABBA product; dashed line desribes the omission error obtained for WFABBA without the temporal filter analysis used for eliminating spurious detections. Vertical bar indicates the overall omission error estimate obtained when all available daytime observations (until 2000 local time) were used to detect the fires mapped with the 30 m resolution imagery at approximately 1030 local time.

Commission Errors

A commission error is here defined as any WFABBA detection with zero 30 m active fire pixels within the GOES pixel footprint or in the immediaty vicinity (i.e., adjacent pixels).

All false detections were associated with contrasting surface temperature conditions between the target pixel and its background (see example on side figure).

A 50% decrease in commission error was found when comparing late morning (~1030 local) to early afternoon (~1330 local) observation hours. This result is partially explained by the thermal inertia of vegetated areas compared to bare soils. This condition induces a larger thermal contrast between the target pixel (a deforested area in this case) and its background (composed of green vegetation) which becomes pronounced near the late morning hours [Schroeder *et al*., submitted].

Fire unrelated commission errors (i.e., GOES pixels without visible scar) estimated for the U.S. and Brazilian Amazonia were nearly identical and accounted for approximately 3% of all WFABBA detections sampled.

We could not identify in our validation data any example of commission error resulting from sub-pixel bright clouds or from solar reflection over water bodies.

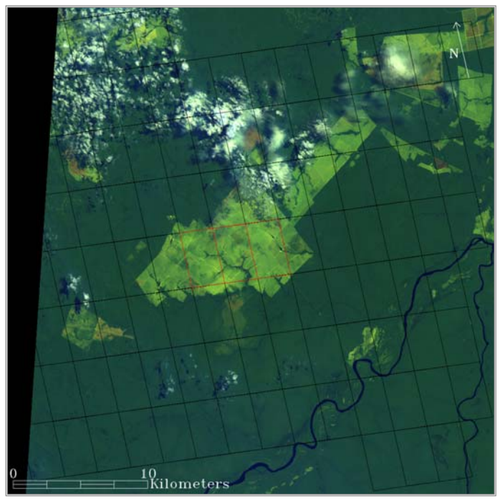

Figure 4: Example of commission error affecting the WFABBA product. Background image corresponds to 30 m resolution ETM+ image from September 26 2002 at 1344 UTC. GOES image grid from the same day at 1345 UTC is displayed in black with WFABBA detections highlighted in red. In this case, the false detections resulted from the large thermal contrast between the warm deforestation area and the cooler green forests surrounding it.

WFABBA versus MOD14

Compared to the MOD14 product, WFABBA detection probability was on average 4× lower. This result contrasts with the 16× factor separating the spatial resolution of the MODIS and GOES instruments.

The broader spectral resolution of channel 2 on the GOES imager appears to facilitate the detection of - in particular - high intensity fires, helping reduce the distance separating the two curves in Figure 5.

Commission error rates for MOD14 and WFABBA were found to be similar over different conditions of percentage tree cover (Figure 6). Major factors inducing false detections in each product were also found to be similar (Table 1).

Fire unrelated commission error rate for MOD14 was approximately 2%, approaching the estimate derived for the WFABBA product.

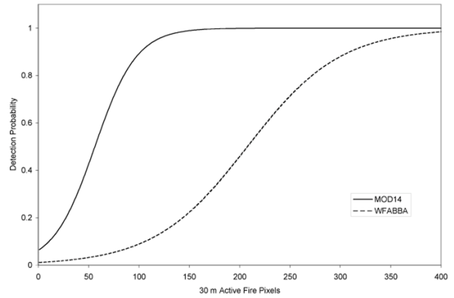

Figure 5: Average detection probability curves for WFABBA and MOD14 products.

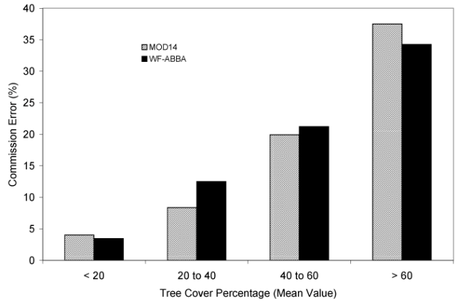

Figure 6: Commission error rates for WFABBA and MOD14 products across Brazilian Amazonia.

Table 1: Classification of commission errors for WFABBA and MOD14 products based on visual interpretation of 30 m resolution imagery.

Product	*Recent Burning (scars visible)*	*Bare Soil*	*Smoldering*	*Spurious detection*
MOD14[1]	79%	12%	8%	1%
WFABBA[2]	75%	19%	6%	-

1 n = 245
2 n = 102

Conclusions

Using 30 m resolution active fire masks produced from ASTER and ETM+, we derived the detection probability curves, and the omission and commission error rates for the WFABBA product. Our results were consistent throughout the two study regions considered. Overall large omission errors (95%) predominated in the instantaneous WFABBA product; however, the use of multiple daytime observations helped reduce those errors to 38%. Commission errors were relatively high in particular over newly deforested areas across Brazilian Amazonia (35%) as a result of high thermal contrast with the adjacent forested areas. False detections were largely associated with recent burning (80%); fire unrelated commission errors accounted for approximately 3% of all WFABBA detections.

Comparison between WFABBA and MOD14 indicated that a relatively small distance separates the detection probability of the two products. Commission errors were found to be similar, a result of the detection algorithm used.

Despite the large omission and commission errors reported, this study is expected to help orient the user community and optmize their use of the WFABBA active fire detection product.

Acknowledgements

This work was funded in part by NOAA's National Environmental Satellite, Data, and Information Services (NESDIS) under grant NESDIS-NESDISPO-2006-2000435 and administered by the Cooperative Institute for Climate Studies (CICS) at the University of Maryland College Park, Maryland. We thank all image analysts at the Satellite Analysis Branch at NOAA/NESDIS for their great support during the implementation of this study.

References

Centro de Previsão do Tempo e Estudos Climáticos (CPTEC), Instituto Nacional de Pesquisas Espacias (INPE), Brazil, URL: http://www.cptec.inpe.br/queimadas
Cooperative Institute for Meteorological Satellite Studies (CIMSS) at the University of Wisconsin, Madison, URL: http://cimss.ssec.wisc.edu/goes/burn/abba.html
Cochrane, M., Alencar, A., Schulze, M.D., Souza Jr., C.M., Nepstad, D.C., Lefebvre, P., & Davidson, E.A. (1999). Positive feedbacks in the fire dynamic of closed canopy tropical forests. , *Science, 284*, 1832-1835.
Csiszar, I., Morisette, J.T., & Giglio, L. (2006). Validation of active fire detection from moderate-resolution satellite sensors: The MODIS example in Northern Eurasia. *IEEE Transactions on Geoscience and Remote Sensing, 44* (7), 1757-1764.
Freitas, S.R., Longo, K.M., Silva Dias, M.A.F., Silva Dias, P.L., Chatfield, R., Prins, E., Artaxo, P., Grell, G.A., & Recuero, F.S. (2005). Monitoring the transport of biomass burning emissions in South America. *Environmental Fluid Mechanics, 5*, 135-167.
Giglio, L., Csiszar, I., Restás, Á., Morisette, J.T., Schroeder, W., Morton, D., & Justice, C. (2008). Active fire detection and characterization with the Advanced Spaceborne Thermal Emission and Reflection Radiometer (ASTER). *Remote Sensing of Environment, accepted*.
Hansen, M. C., DeFries, R. S., Townshend, J. R. G., Sohlberg, R., Dimiceli, C., & Carroll, M. (2002). Towards an operational MODIS continuous fields of percent tree cover algorithm: examples using AVHRR and MODIS data. *Remote Sensing of Environment, 83*, 303-319.
Hazard Mapping System (HMS), NOAA/NESDIS, Camp Springs, URL: http://www.ssd.noaa.gov/PS/FIRE/hms.html
Keeley, J. E., Fotheringham, C. J., & Morais, M. (1999). Reexamining fire suppression impacts on brushland fire regimes. *Science, 284 (11)*, 1829-1832.
Morisette, J., Giglio, L., Csiszar, I., & Justice, C. (2005). Validation of the MODIS active fire product over Southern Africa with ASTER data. *International Journal of Remote Sensing, 26*, 4239-4264.
Prins, E.M., & Menzel, W. P. (1994). Trends in South American biomass burning detected with the GOES VAS from 1983-1991. *Journal of Geophysical Research, 99* (D8), 16719-16735.
Schroeder, W., J. T. Morisette, I. Csiszar, L. Giglio, D. Morton, & C. Justice (2005). Characterizing vegetation fire dynamics in Brazil through multisatellite data: Common trends and practical issues, *Earth Interactions, 9*, Paper 13.
Schroeder, W., Prins, E., Giglio, L., Csiszar, I., Schmidt, C., Morisette, J., Justice, C., & Morton, D. (2008). Validation of GOES and MODIS active fire detection products using ASTER and ETM+. *Remote Sensing of Environment, accepted*.
Setzer, A.W., & M.C. Pereira (1991), Amazonia biomass burnings in 1987 and an estimate of their tropospheric emissions, *Ambio, 20* (1), 19-22.